applied sciences

MDPI

Article

Study on the Direct Current Breakdown Characteristics and Influence of Electric Field Distribution in Water Droplets in Rod–Plate Air Gaps

Jianli Zhao [1], Zhaoyang Du [2], Jiankun Zhao [1], Song Fu [3] and Bin Cao [3,*]

[1] Inner Mongolia Power (Group) Co., Ltd., Inner Mongolia Power Research Institute Branch, Hohhot 010020, China; jianli791026@126.com (J.Z.); zjk2008123zjk@163.com (J.Z.)
[2] College of Electrical Power, Inner Mongolia University of Technology, Hohhot 010051, China; dzy1997wjs@163.com
[3] Tsinghua University Shenzhen International Graduate School, Shenzhen 518071, China
* Correspondence: huhu0512@126.com; Tel.: +86-13128920172

Abstract

This study primarily simulates the flashover phenomenon between the metal fittings (rods) and the skirt surface (plates) of insulators when water droplets traverse between them under heavy rain conditions. High-speed cameras recorded droplet deformation and breakdown processes, while electric field simulation software modeled the air gap's electric field distribution. The effects of air gap length, axial position of the water droplet, droplet conductivity, droplet diameter, and voltage polarity on the DC breakdown voltage were analyzed. Results indicate that a larger air gap leads to a greater reduction in droplet breakdown voltage and lower electric field uniformity. The breakdown voltage is essentially independent of changes in the axial position of the droplet and the droplet's conductivity. The breakdown voltage exhibits no significant correlation with droplet diameter. Droplets rarely break down when voltage is applied to the electrodes, indicating that flashover at the low-voltage end of insulators during rainfall occurs infrequently. This research holds significant importance for elucidating the flashover mechanisms of water droplets at both ends (high-voltage and low-voltage) of the insulators and for guiding the design of external insulation for power equipment.

Keywords: water droplets; air gaps; flashover; breakdown voltage; electrical field uniformity

1. Introduction

The intensification of global climate change has led to frequent extreme rainfall events, and the phenomenon of insulator rain flashover poses a serious threat to power system safety, becoming a significant challenge for the secure operation of high-voltage transmission lines [1–5].

The effect of water droplets on gap breakdown characteristics under AC voltage has been well established. Scholars have conducted systematic research on various influencing factors. Regarding electrode structure and droplet parameters, Chen et al. found that increasing the diameter of fine mist droplets enhances the maximum electric field between rod–plate electrodes [6]. Danikas et al. further indicated that droplet position exerts a greater influence on flashover voltage than droplet volume [7]. Concerning environmental and dielectric parameters, Jiang et al. revealed that breakdown voltage decreases with

Check for updates

Academic Editor: Gerard Ghibaudo

Received: 21 November 2025
Revised: 30 December 2025
Accepted: 1 January 2026
Published: 16 January 2026

Copyright: © 2026 by the authors. Licensee MDPI, Basel, Switzerland. This article is an open access article distributed under the terms and conditions of the Creative Commons Attribution (CC BY) license.

increasing rainfall intensity and conductivity, while it increases with rising ambient temperature [8]. Subsequent studies also indicate that the flashover voltage decreases significantly when the resistivity of rainwater is low, while it exhibits a saturation trend when the resistivity is high [9]. Collectively, these studies demonstrate that under AC voltage conditions, the air gap length, water droplet characteristics (volume, position), conductivity, and rainwater resistivity are key factors influencing the breakdown voltage.

Research under DC voltage conditions has focused more on rod–rod electrode configurations. Research by Wu and Cao et al. indicates that the impact of water droplets on DC breakdown voltage correlates with air gap length—shorter gaps exhibit more pronounced voltage reduction [10]. Additionally, under lightning impulse voltages, Liu et al. observed that introducing a metal plate lowers breakdown voltage in rod–plate–rod gaps compared to rod–rod gaps, with this phenomenon being voltage-polarity dependent [11]. Taniguchi et al. compared saturation characteristics across different gaps, noting that under long gaps, the flashover voltage of rod–plate gaps may be lower than that of rod–rod gaps [12].

Notably, existing conclusions regarding the DC breakdown characteristics of short rod–plate gaps under rainy conditions exhibit inconsistencies and research gaps. Some studies, such as those by Jiang and Nazemi and Hinrichsen, indicate that the DC discharge voltage of short rod–plate air gaps under wet conditions is even slightly higher than under dry conditions, with light rain having minimal impact [13,14]. However, these studies have not yet deeply revealed the specific influence mechanisms of charge accumulation and local electric field distribution on the breakdown process of rod–plate gaps under DC voltage. Concurrently, Swift theoretically proposed that severe deformation of water droplets on fully hydrophobic surfaces may trigger flashover [15]. Jie et al., using a sphere-to-sphere air gap model, suggested that the reduction in breakdown voltage amplification is attributed to field distortion and increased gap distance [16]. However, this qualitative analysis lacks sufficient experimental support in the context of DC rod-to-plate short air gaps.

In summary, existing research has accumulated substantial findings on the influence of water droplets on AC flashover voltage (rod-to-plate gaps) and DC flashover voltage (rod-to-rod gaps). Nevertheless, systematic and in-depth studies remain scarce regarding the breakdown dynamics, charge accumulation effects, and specific electric field distortion mechanisms of water droplets in short rod-to-plate gaps under DC voltage conditions. This gap hinders accurate assessment of the external insulation performance of DC transmission lines under actual heavy rain conditions. Therefore, this study aims to address this research deficiency by conducting experimental observations and mechanism analysis to investigate the breakdown process of water droplets in rod-to-plate short gaps under DC voltage. It seeks to clarify the flashover mechanism and analyze the specific influence of electric field distribution on flashover voltage.

2. Experimental Test Setup and Methods

2.1. Experimental Test Setup

This study investigates the air gap breakdown mechanism when liquid media traverse non-uniform electric field spaces, focusing on establishing a multi-physics coupling analysis system for water droplets and electric fields. The experimental platform employs a self-designed rod–plate electrode dynamic control system and high-voltage electric field loading apparatus, enabling investigation of the influence patterns of air gap parameters and liquid medium interference on discharge channel development. As shown in Figure 1, this experiment utilizes a rod–plate electrode configuration (air gap), where the rod electrode consists of a sharp steel needle tip with a diameter of 1.0 mm, and the plate electrode comprises a polished copper plate (diameter 8.0 cm). The air gap distance is dynamically controlled via a unilateral mechanical adjustment system, with a range from 4.0 mm to

20.0 mm. A water droplet generation device is positioned 10.0 cm above the central axis of the electrodes. A water-dropping mechanism stably generates water droplets that continuously fall under gravity through the center of the gap between the rod and plate. The device drips at a rate of one droplet per second. This precisely simulates the disturbance process of a liquid medium in a non-uniform electric field.

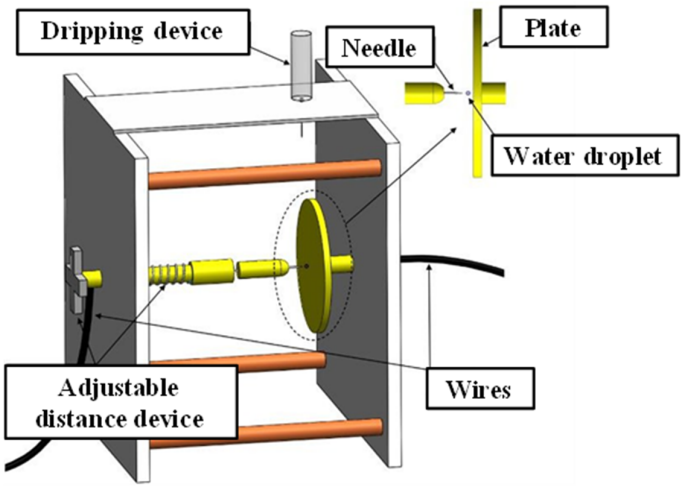


Figure 1. Experimental Test Setup.

This experiment employs a high-voltage DC regulated power supply system. The power supply's rated input parameters are AC 220.00 V/3.00 A, while the output provides a stable negative high voltage rated at DC −50.00 kV/15.00 mA. The voltage signal was coupled to a digital storage oscilloscope via a high-voltage differential probe (1000:1 attenuation ratio) for waveform acquisition and recording. Noise in the actual output voltage waveform resulted from the oscilloscope's sampling error. The experimental setup employed a bipolar system, with the high-voltage output selectively applied to either the rod electrode or the plate electrode. The corresponding non-energized electrode was reliably grounded through a low-impedance path.

This experiment employs a high-speed camera (frame rate $\geq$ 10,000 fps, spatial resolution $\geq$ 1920 $\times$ 1080 pixels) to dynamically capture water droplet dielectric breakdown phenomena. To enhance high-speed imaging quality, an LED light source is configured for dark-field illumination.

2.2. Experimental Testing Method

This experimental system investigates the dielectric breakdown characteristics of water droplets and their multiphysics coupling mechanisms. A two-dimensional multiphysics coupling model was constructed through experimental and finite element simulation analyses to examine droplet morphology and surrounding electric field variations. Core variables included: rod–plate electrode spacing (4.0–20.0 mm), axial release position of the water droplet, voltage polarity configuration, water droplet diameter (precisely controlled via microfluidic syringe), and conductivity. The experimental design employed syringe needles of varying diameters to generate droplets of different sizes, supplemented by gradient-concentration NaCl electrolyte solutions.

The DC voltage ramped at 0.10 kV/s. An oscilloscope triggered upon rod–plate air gap breakdown, recording the voltage waveform at breakdown. For clarity, negative DC high voltage applied to the rod electrode is termed rod-side voltage, while applied to the plate electrode is termed plate-side voltage, simulating breakdown between the high-voltage end and low-voltage end fittings and the skirt of an insulator. The experiment employed

a single-variable control approach. Based on the experimental variables, the process was first decomposed into typical water droplet breakdown stages. Subsequently, four sets of operating condition experiments were conducted: air gap length experiments, water droplet axial position experiments, water droplet conductivity experiments, and water droplet diameter control experiments. Finally, a discussion and analysis were performed. The first two sets of operating condition experiments were configured with different voltage levels, each repeated five times to calculate the average breakdown voltage.

3. Experimental Results

3.1. Decomposition of the Typical Water Drop Breakdown Process

Experimental parameters selected: water droplet conductivity 500.00 μS/cm, droplet diameter of 1.9 mm, and rod–plate gaps of 4.0 mm, 10.0 mm, and 15.0 mm. The experimental configuration employed rod–plate voltage. This illustrates three typical breakdown modes of water droplets under air gaps.

Small gap droplet breakdown: At an air gap length of 4.0 mm, the dynamic evolution of the droplet occurs in four distinct stages, as illustrated in Figure 2. (a) Free fall stage: Subjected to gravitational acceleration and Coulombic force [17], the droplet forms a quasi-spherical shape after detaching from the dispenser, exhibiting minimal displacement. (b) Falling deformation stage: Upon entering the strong electric field region of the air gap, the droplet undergoes an expansion-contraction effect due to the intense electric field, transforming from a quasi-spherical to a conical shape. (c,d) Breakdown development stage: When the droplet aligns with the central axis of the rod–plate electrodes, it approaches the high-field concentration zone near the tip of the rod electrode. An arc originates from the rod electrode, propagates along the liquid–gas interface, and ultimately reaches the plate electrode. (e,f) Breakdown termination stage: The droplet exits the high-field region, displaces toward the plate electrode, and ultimately assumes a quasi-hemispherical shape before impacting the plate.

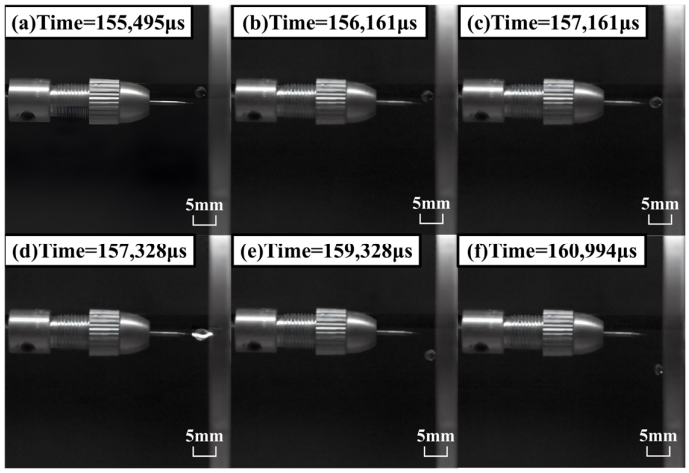


Figure 2. Droplet breakdown in a small gap (rod–plate gaps of 4.0 mm).

Water drop normal breakdown: When the air gap length is 10.0 mm, the dynamic evolution of the water drop is divided into three stages, as shown in Figure 3. (a,b) Falling deformation stage: Due to the stronger breakdown voltage at this point, the Coulomb force acting on the water drop within the air gap intensifies, causing slight drift and transforming it into a flattened conical shape. (c,d) Breakdown development stage: The flattened conical shape reduces the air gap between the rod and plate, enabling the arc to simultaneously connect rod-water droplet-plate and form a conductive path. (e,f) Breakdown termina-

tion stage: After the droplet breakdown concludes, it assumes an irregular shape under the influence of the stronger residual electric field from the plate electrode. Due to the distance between the rod and plate, the droplet regains a quasi-spherical form during its displacement toward the plate and subsequently impacts it.

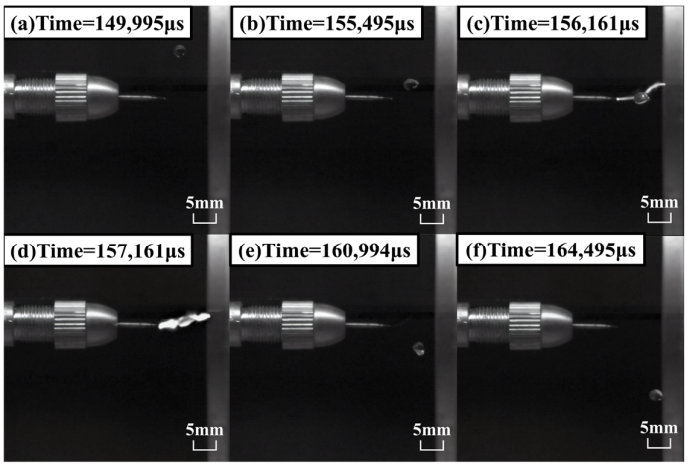


Figure 3. Normal-state breakdown of water droplets (rod–plate gaps of 10.0 mm).

Water drop breakdown along the plate electrode: At an air gap length of 15.0 mm, the dynamic evolution of the water drop is divided into three stages. As shown in Figure 4. (a–d) Falling deformation stage: Under the influence of the strong electric field, the water droplet gradually approaches the plate electrode as it enters the air gap region. Its shape transitions from quasi-spherical to elliptical and then to a flattened conical form as it descends along the plate. Near the strong field region close to the center axis of the rod–plate electrodes, the droplet undergoes oscillations. where the phase relationship between droplet oscillations and the electric field governs corona initiation [18]. (e) Breakdown development stage: An arc forms from the rod electrode, connecting the droplet surface to the plate electrode. (f) Breakdown termination stage: The droplet assumes a quasi-hemispherical shape and slides down the plate.

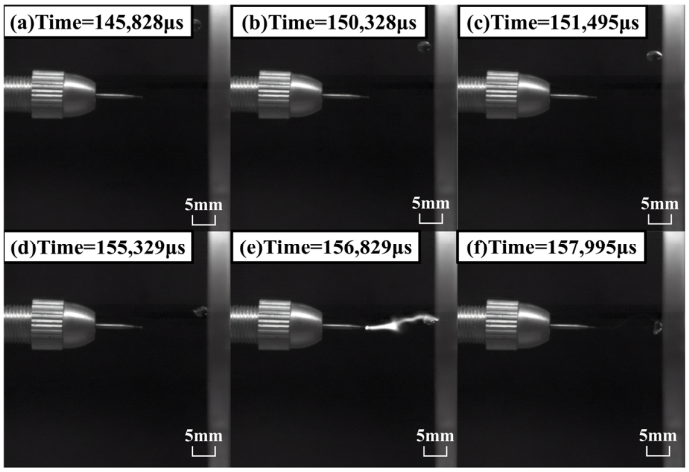


Figure 4. Droplet breakdown along plate electrode (rod–plate gaps of 15.0 mm).

Based on the above analysis, 4 mm short gap: The electric field is extremely strong, with the water droplet primarily governed by vertical electric forces. Deformation occurs directly, and the arc develops strictly along the liquid–gas interface, indicating that the concentrated electric field at the interface is the primary cause of breakdown. After ter-

mination, surface tension rapidly restores the droplet to a quasi-hemispherical shape. A 10 mm medium gap: moderate electric field strength. Water droplet exhibits noticeable horizontal drift, deforming into a flattened cone shape while simultaneously reducing the local air gap. During breakdown, the arc simultaneously connects both ends of the droplet, indicating it has become a direct conductive channel between electrodes. Residual electric fields cause irregular post-breakdown morphology. A 15 mm long gap: weaker electric field causes significant horizontal drift and oscillation toward the electrode plates due to the horizontal component of the electric field. Deformation progresses more slowly. Breakdown occurs with an arc connecting only the droplet surface and the plate, reflecting the preferential selection of discharge paths in long gaps. The typical breakdown process of a water droplet can be summarized as droplet descent, droplet deformation, droplet breakdown, and droplet contact with the electrode plate. During this process, the droplet deformation state is predominantly conical; breakdown primarily occurs as an arc along the droplet surface or as an arc connecting both ends of the droplet surface; the droplet contacts the electrode plate in a conical shape during breakdown, transforming into a quasi-hemispherical or quasi-spherical shape after breakdown.

To study breakdown voltage waveforms, the water droplet breakdown was initiated at time 0.00 ms. The recovery time for breakdown at the small gap was set to 100.00 ms, with no abrupt changes occurring during this period. The breakdown voltage recovery times for normal droplet breakdown and droplet breakdown along the plate electrode were 788.41 ms and 1134.34 ms, respectively, with abrupt changes occurring at 702.08 ms and 718.73 ms during recovery.

As shown in Figure 5, comparing the breakdown voltage waveforms of the three typical droplet cases reveals that higher breakdown voltages result in greater voltage reduction and longer recovery times. The duration of the sudden change during breakdown voltage recovery correlates with the length of the droplet breakdown process; longer breakdown processes yield longer sudden change durations during recovery.

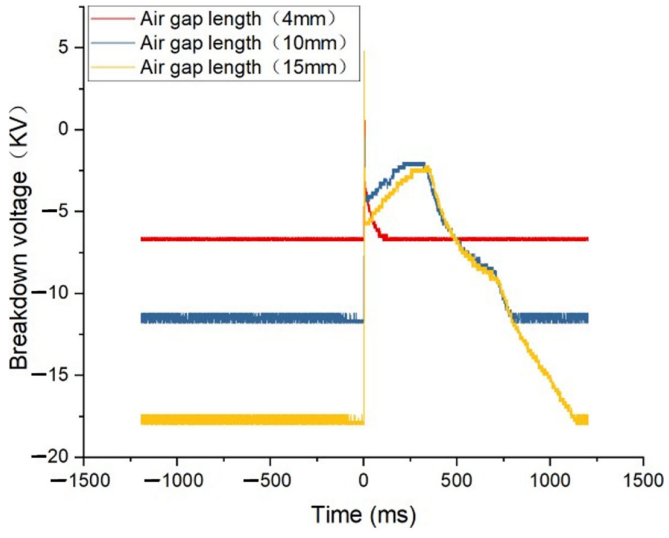


Figure 5. Typical water drop breakdown voltage waveforms for rod–plate air gap lengths of 4.0 mm, 10.0 mm, and 15.0 mm.

3.2. *Effect of Air Gap Length*

The experimental conditions selected were water droplet conductivity of 500.00 μS/cm, droplet diameter of 1.9 mm, and air gap length varying from 4.0 mm to 20.0 mm.

Figure 6 illustrates the influence of air gap length on breakdown voltage for both air gap breakdown and water droplet breakdown under rod electrode voltage and plate electrode voltage conditions.

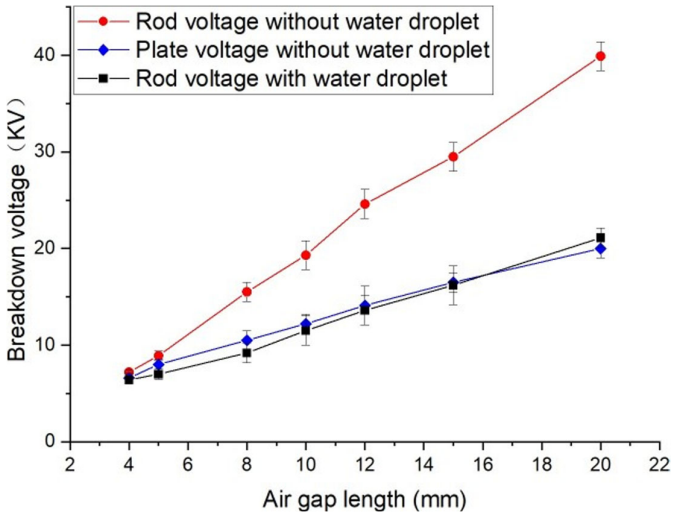


Figure 6. Effect of air gap length on breakdown voltage when applying rod and plate voltages.

Under rod electrode voltage, at air gap lengths of 4.0 mm and 5.00 mm, the average breakdown voltages without water droplets were 7.20 kV and 8.90 kV, respectively, while those with water droplets were 6.40 kV and 7.00 kV. At an air gap length of 8.0 mm, the average breakdown voltage without water droplets was 15.50 kV, while with water droplets it was 9.20 kV. Breakdown voltage increased with air gap length, and the breakdown voltage with water droplets was lower than that without.

Under plate electrode voltage, the breakdown voltage without water droplets increases linearly across different air gap lengths. This value is lower than the breakdown voltage without water droplets under rod electrode voltage. Its growth trend resembles that of breakdown voltage with water droplets under rod electrode voltage, though no clear pattern exists between them. Under plate electrode voltage, air gap breakdown predominates with negligible droplet breakdown. However, droplets in the air gap exhibit deformation and displacement patterns similar to those under rod electrode voltage. Droplet breakdown behavior under plate electrode voltage will be analyzed in Section 4.

Figure 7 illustrates the relationship between air gap length and the average breakdown voltage drop rate. When the air gap length ranges from 4.0 mm to 8.0 mm, the drop rate varies from 11.11% to 40.64%; for air gaps between 8.0 mm and 20.0 mm, the drop rate ranges from 40.64% to 47.11%. It can be observed that the average breakdown voltage drop rate generally increases with increasing air gap length. Under plate electrode voltage conditions, achieving air gap breakdown is easier than applying voltage to rod electrodes at different gaps, and water droplets generally do not participate in arc development during their descent.

3.3. Effect of Water Drop Axial Position on Breakdown Voltage

Experimental conditions: Water droplet conductivity 500.00 μS/cm, droplet diameter 1.9 mm, fixed air gap length 20.0 mm. Axial positions (droplet-to-electrode distance) tested: 4.0 mm, 8.0 mm, 12.0 mm, 16.0 mm. The droplet positions are shown in Figure 8.

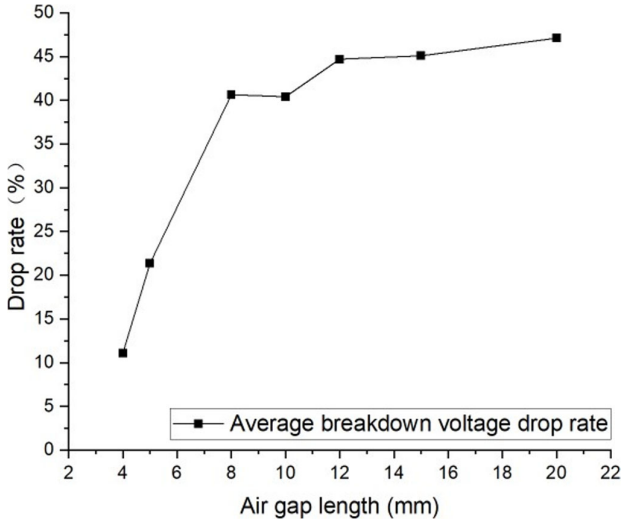


Figure 7. Relationship between air gap length and average breakdown voltage decrease rate when applying rod voltage.

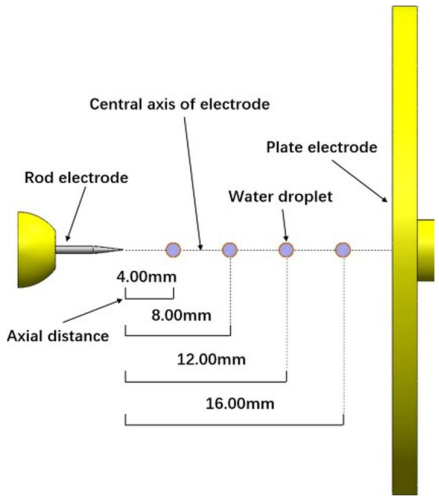


Figure 8. Schematic of water droplet positions.

Figure 9 illustrates the effect of axial water droplet position on breakdown voltage under rod electrode voltage and plate electrode voltage in a fixed air gap.

Under rod electrode voltage, the average breakdown voltage without a water droplet was 39.90 kV. With water droplets present, the average breakdown voltage remains similar. When the axial position of the water droplet changes, the average breakdown voltage varies between 21.10 kV and 22.00 kV. Compared to the condition without water droplets, the average breakdown voltage reduction ranges from 44.86% to 47.11%. When the water droplet falls within a fixed air gap, the breakdown voltage trend remains stable as the droplet's axial position changes.

Under plate electrode voltage, the average breakdown voltage without water droplets was 20.00 kV, which was lower than the average breakdown voltage under rod electrode voltage.

Water droplets falling at different axial positions all experience breakdown near the plate electrode side, with breakdown locations occurring at similar axial distances. When droplets fall from axial positions (a) 4.0 mm to (d) 16.0 mm, the breakdown location gradually transitions from below the central axis to above it, as shown in Figure 10.

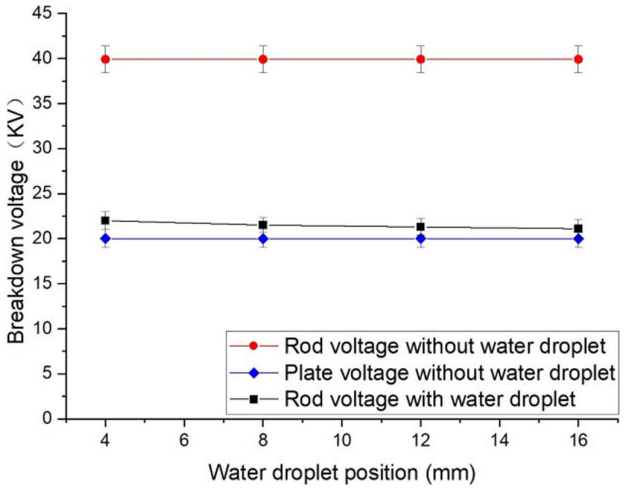


Figure 9. Effect of axial position of water droplet on breakdown voltage when applying rod and plate voltage.

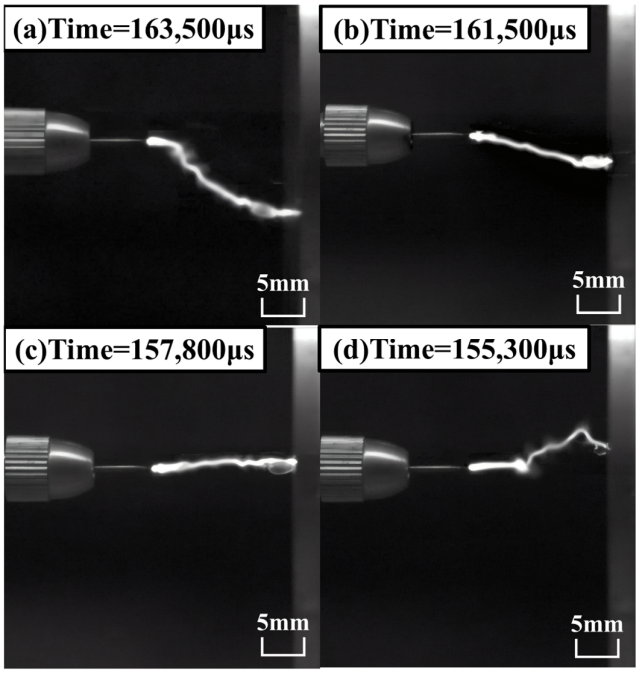


Figure 10. Relationship between axial droplet position and breakdown position when applying rod Voltage. Axial droplet position: (**a**) 4.0 mm; (**b**) 8.0 mm; (**c**) 12.0 mm; (**d**) 16.0 mm.

Within the rod–plate gap, applying high voltage to the rod electrode creates an extremely high electric field strength near its tip, ionizing the air and generating corona discharge. This produces a large number of ions with the same polarity as the rod electrode. During injection, the water droplet is initially uncharged. As it traverses the gap, it captures these ions and becomes charged, acquiring the same polarity as the rod electrode. The charged droplet experiences a Coulomb force in the electric field: if the rod electrode is positive, the electric field direction points from the rod toward the plate, causing the positively charged droplet to be attracted toward the plate. If the rod electrode is negative, the electric field direction points from the plate toward the rod, causing the negatively charged droplet to be attracted in the opposite direction of the electric field, also toward the plate. Therefore, regardless of the rod electrode's polarity, the droplet always moves toward the flat plate. Additionally, the droplet may experience a dielectric force due to polarization. However, this force typically points toward the rod tip where the electric

field is stronger, which contradicts the observed phenomenon. Therefore, the primary mechanism is determined to be the Coulomb force acting on the charged droplet [17].

This occurs because as the water droplet descends near the rod electrode, it acquires a high potential close to the rod electrode due to capacitive coupling, effectively becoming an equivalent electrode closer to the plate. At this point, the region of strongest electric field within the entire gap shifts from the rod tip to the water droplet. Breakdown is thus initiated first at this point (the location nearest the plate with the highest electric field strength) resulting in the breakdown position appearing low. Conversely, when the droplet moves farther away, the strongest electric field region lies between the rod tip and the droplet, causing the breakdown initiation point to shift upward. This phenomenon essentially allows the droplet, acting as a conductor, to dominate the core region of electric field distortion through its position, thereby precisely controlling the initiation point of the discharge.

Essentially, the electric field force governs the droplet's convergence path and breakdown timing, while the initial position determines the spatial geometry of this path. Together, they constrain the spatial distribution of breakdown points.

When the plate voltage is applied up to the air gap breakdown voltage, the elongation of the air gap causes the region around the water droplet to reach a uniform electric field. This prevents the critical electric field strength for air ionization from being attained, thus inhibiting droplet breakdown. As the droplet falls between axial positions 4.0 mm and 12.0 mm, it undergoes minimal deformation during descent. Its displacement path within the air gap converges toward the plate direction from the initial drop position. When the droplet falls at axial position 16.0 mm, it descends along the electrode plate and undergoes multiple irregular deformations due to the strong electric field on the plate surface during its descent. Take the elliptical deformation of the water droplet as an example, as shown in Figure 11.

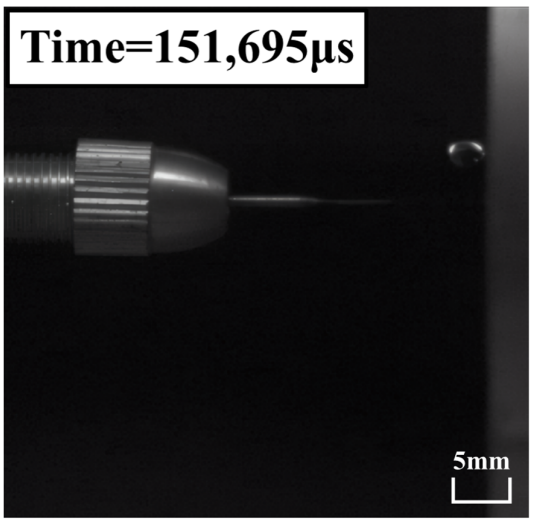


Figure 11. Elliptical deformation of water droplet.

Based on the above experimental analysis, it is evident that at a fixed gap, the axial position of the water droplet has little effect on the breakdown voltage, and the breakdown voltage can be significantly reduced at different axial positions. The shorter the axial distance between the starting point and the final landing point of the droplet, the lower the height at which the droplet undergoes breakdown in the air gap; however, this is unrelated to the axial position of the droplet's breakdown within the air gap.

When the applied voltage reaches the overall breakdown threshold for the long air gap, the electric field distribution between the plates tends toward uniformity. At this point, the

field strength in the region containing the water droplet falls below the threshold required for significant polarization deformation and ionization initiation, thereby suppressing the droplet breakdown mechanism. In the axial mid-region (4.0–12.0 mm), the droplet resides within a relatively uniform electric field. The electric force acting upon it is weak and primarily directed toward the plates, resulting in only directional drift without significant deformation. At the axial position near the electrode (16.0 mm), the droplet enters the strong field region at the edge of the electrode surface. The high electric field gradient in this area causes significant changes in the surface charge distribution of the droplet. Consequently, it experiences alternating electric forces, leading to irregular deformation and vibration.

Experiments demonstrate that droplets do not break down under plate electrode voltage. When the axial distance is short, the droplet's movement path (toward the plate electrode) is affected, while its morphological changes remain unaffected. When the axial distance is long, the droplet's movement path (along the plate electrode) remains fixed, primarily causing continuous morphological distortion.

3.4. Effect of Water Drop Conductivity

The experimental conditions selected were as follows: water droplet diameter of 1.9 mm, fixed air gap length of 10.0 mm, and water droplet conductivity set to 20.34, 180.77 μS/cm, and 1.12, 5.49, 9.82 mS/cm.

As shown in Figure 12, when the water droplet conductivity changes from the μS/cm level to the mS/cm level, there is no obvious pattern in its effect on the breakdown voltage. Within this range of conductivity variation, the dielectric polarization characteristics of the water droplet may be sufficient to cause significant deformation under strong electric fields, thereby inducing intense field distortion. Simultaneously, arc development relies on gas ionization at the gas–liquid interface, a process governed by electric field strength and droplet geometry, while exhibiting relative insensitivity to the droplet's intrinsic conductivity.

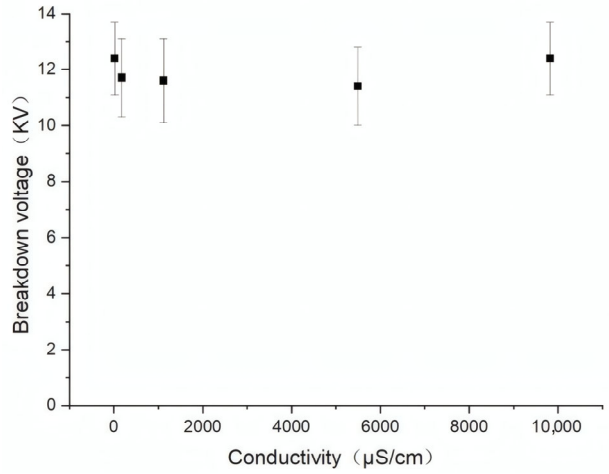


Figure 12. Effect of water droplet conductivity on breakdown voltage when applying rod voltage.

3.5. Effect of Water Drop Diameter

The operating parameters selected for this experiment were: water droplet conductivity of 500.00 μS/cm, water droplet diameters of 1.9 mm, 2.2 mm, 2.5 mm, and 3.0 mm, and an air gap length of 10.0 mm.

The average breakdown voltages were 11.50 kV and 12.60 kV for droplets of 1.9 mm and 2.20 mm diameter, respectively, and 10.40 kV and 10.50 kV for droplets of 2.5 mm and 3.0 mm diameter, respectively, as shown in Figure 13.

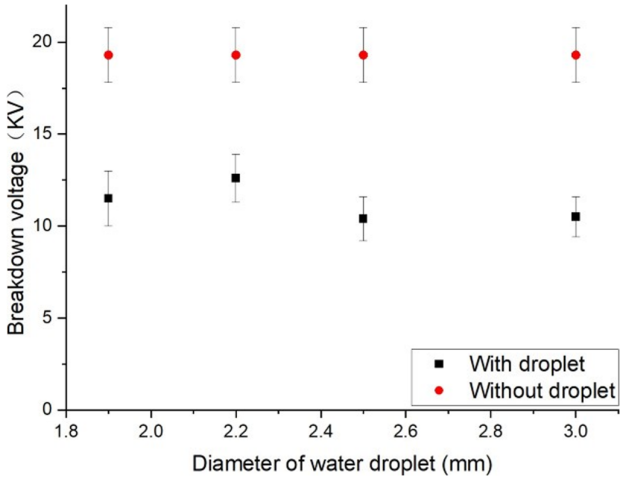


Figure 13. Effect of water droplet diameter on breakdown voltage when applying rod voltage.

The relationship between droplet diameter and breakdown voltage is not pronounced. In highly non-uniform electric fields, the spatial potential and field strength distribution are dominated by electrode configuration. In strong electric fields, droplets of different diameters undergo polarization stretching, leading to similar local field strength concentrations and thus reduced breakdown voltage differences.

This phenomenon indicates that under the experimental conditions, the distribution and intensity of the external electric field are the primary controlling factors for breakdown. The influence of droplet size is masked by stronger electric field inhomogeneity.

4. Discussion

4.1. Discussion on the Uniformity of the Electric Field

To investigate the effects of water droplets in air gaps on breakdown voltage and electric field generation, COMSOL Multiphysics 6.3 finite element simulation software was employed to analyze electric field distributions.

In simulation analysis, considering that the shape and position of the water droplet differ when it passes through the central axis of the electrode plate during its descent, the use of two-dimensional axisymmetric finite element analysis fails to achieve ideal results. Simultaneously, three-dimensional simulation has significant limitations in modeling fluid descent, with simulation results falling short of practical standards. Therefore, two-dimensional plane finite element analysis is employed as the analytical method, capable of simulating the morphological changes induced by the electric field during the water droplet's descent. The physical experiment and simulation comparison of water droplets falling in the air gap are shown in Figure 14.

Studies have shown that as the deformation degree of the droplet increases, the breakdown voltage also rises [19]. Incorporating the electric field non-uniformity coefficient η into the analysis allows representation of the intensity by which droplets alter electric field uniformity within the air gap. The value of η enables assessment of droplet influence on the air gap electric field. η is defined as:

$$\eta = \frac{E_{max}}{E_{avg}} \tag{1}$$

$$E_{avg} = \frac{U_{gap}}{d} \tag{2}$$

where E_{max} is the maximum electric field value; E_{avg} is the average electric field value; U_{gap} is the applied voltage between electrodes; and d is the air gap length.

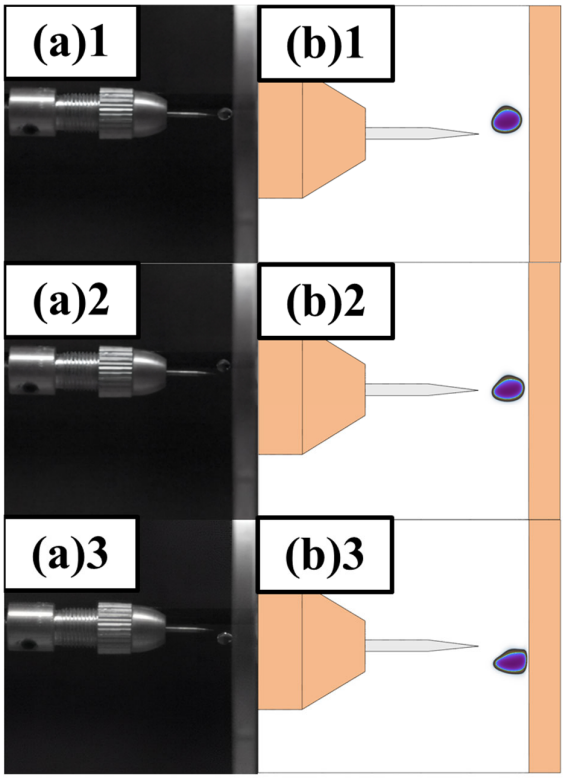


Figure 14. Experimental and simulated comparisons. (**a**) Left image: Experimental electrode; (**b**) Right image: Simulated electrode.

Based on a comparison between physical measurements and simulations, COMSOL Multiphysics finite element analysis software was used to calculate the electric field distribution under simulated rod-to-rod voltage conditions for scenarios with no water droplets and three different scenarios with water droplets in the air gap. Taking the simulation results for a 4.0 mm air gap length as an example, Table 1 illustrates the variation in the air gap electric field non-uniformity coefficient across the four scenarios.

Table 1. Variation in the electric field non-uniformity coefficient between electrodes when applying rod voltage.

No.	Water Droplet Shape	Non-Uniformity Coefficient of Electric Field η
1	Without water droplet	2.75
2	Near-spherical water droplet	2.79
3	Conical water droplet	4.28
4	Conical water droplet contact plate	3.48

The results in Table 1 indicate that the presence of water droplets increases η. The dynamic changes generated during the droplet's descent through the air gap enhance the electric field inhomogeneity, with droplet deformation having the most significant impact on field uniformity. This deformation is the primary cause of the altered breakdown voltage.

4.2. Discussion on Droplet Breakdown at Plate Voltage

After conducting a large number of experiments and analyses, under the plate electrode voltage, the probability of water droplets undergoing breakdown is extremely low, but breakdown can still occur. Based on the video footage captured by the high-speed camera and using the electric field simulation software for analysis.

The breakdown process of water droplets under plate electrode voltage is illustrated in Figure 15. It was observed that breakdown only occurs when the droplet contacts the plate electrode, while no breakdown occurs in the air gap. (a,b) depict the displacement and deformation of the water droplet as it enters the air gap. This behavior stems from the Coulomb force exerted by the electric field on the droplet and the non-uniform electric field distribution caused by the asymmetric electrode structure. Regardless of voltage polarity, the strong electric field zone near the rod electrode consistently drives the ionization process toward the weaker field region (the plate electrode). (c) demonstrates that breakdown predominantly occurs in the air gap, unrelated to the droplet, and (d) shows the scenario during droplet breakdown, where branching of the electric arc occurs upon breakdown.

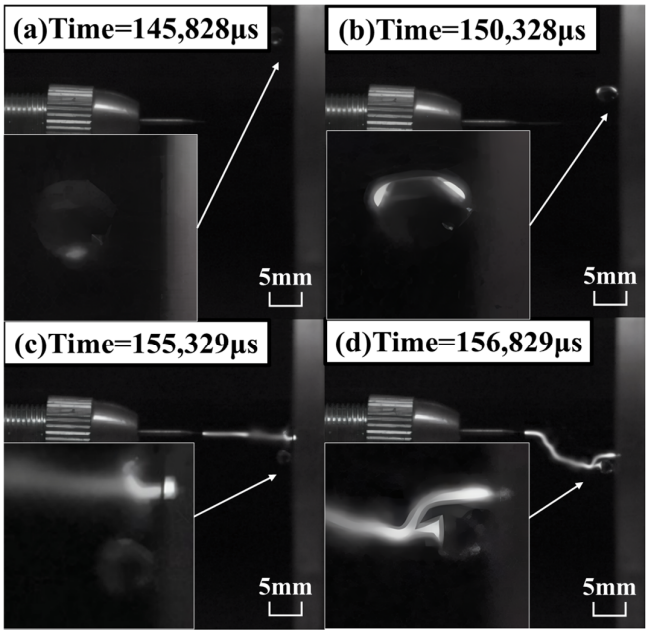


Figure 15. Droplet breakdown process under plate voltage.

COMSOL Multiphysics Simulation software analyzed the electric fields at the droplet-contacting and non-contacting electrodes. From the electric field line distribution in the air gap, the field lines near the droplet contact the plate are denser, while other regions are sparser. The overall trend of the field lines is from the rod electrode through the droplet surface to the plate electrode, as shown in Figure 16. The electric field distribution on the droplet surface reveals a non-symmetrical double-peak configuration. Unlike the rod electrode voltage scenario, the right peak is slightly higher, and the field collapse region exhibits irregularities, as shown in Figure 17.

When the droplet contacts the plate electrode, the electric field distribution on the plate surface becomes non-uniform. Multiple points of fluctuating electric field strength simultaneously form on the droplet surface. Dense space charges repel each other during diffusion, ultimately dissipating energy through branching arc paths. This generates bifurcated arcs and an irregular electric field curve, causing variations in the droplet's breakdown voltage and potentially leading to breakdown under these conditions.

When the water droplet does not contact the plate electrode, the electric field distribution on the plate surface is uniform. This eliminates the surface field strength distortion at the droplet tip, causing the electric field concentration effect to fail. The electric field variation trend becomes smoother, and the electric field strength is relatively weaker compared to when the droplet contacts the plate. At this point, the water droplet does not experience breakdown.

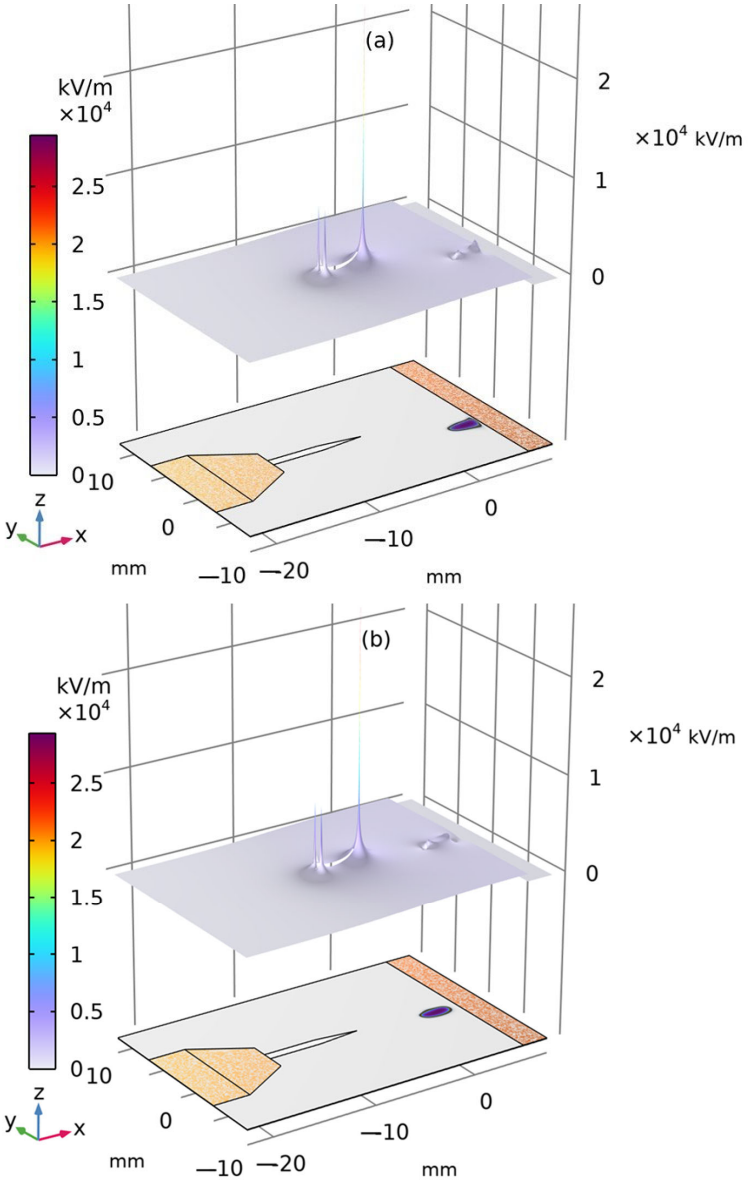


Figure 16. Electric field line distribution in the air gap between the rod and plate when applying plate voltage. (**a**) Water droplets contact the electrode of the plate. (**b**) Water droplets do not touch the electrode of the plate.

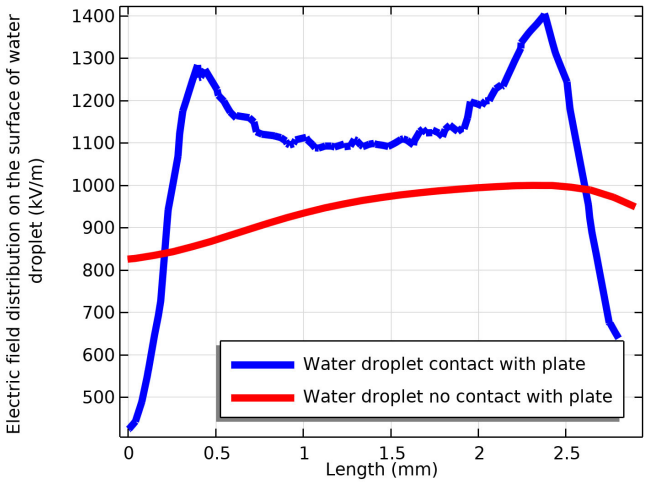


Figure 17. Comparison of droplet surface electric field distribution under plate voltage.

5. Conclusions

This study observed the deformation of water droplets and the breakdown phenomenon occurring as they pass through a rod–plate gap (air gap) using high-speed camera imaging. Through experiments and finite element simulation analysis, the following conclusions can be drawn:

1. The breakdown voltage of the rod–plate gap when water droplets are present is lower than that when there are no water droplets. Moreover, the greater the gap length, the greater the reduction in breakdown voltage, and the lower the uniformity of the electric field.
2. The typical breakdown process of a water droplet can be summarized as: droplet descent, droplet deformation, droplet breakdown, and droplet contact with the electrode plate. During descent, when the electric field strength is high, the droplet undergoes morphological changes, transforming from a near-spherical shape to a conical shape, and subsequently to a more irregular shape. These morphological changes are often accompanied by vibrations on the droplet's surface.
3. With a fixed air gap length (20.0 mm), droplet breakdown consistently occurs near the electrode plate side. Regardless of the axial position from which the droplet falls, the breakdown voltage remains relatively stable.
4. For longer air gaps (10.0 mm), the influence of droplet conductivity on breakdown voltage is negligible. When droplet conductivity changes, the arc path predominantly involves series connection between the droplet and the arc. The relationship between breakdown voltage and droplet diameter is not clearly defined.
5. When plate voltage is applied, water droplets rarely break down. Breakdown occurs only rarely when the droplet contacts the plate electrode, and the breakdown arc exhibits branching.

This study reveals fixed patterns of water droplet-induced discharges, providing evidence for the flashover mechanism of water droplets at both ends of insulators. Phenomena such as branched arcs can serve as criteria for identifying specific discharge types. Within a certain range, the influence of water droplet conductivity and diameter on breakdown voltage is insignificant. This indicates that when evaluating water droplets with complex compositions (variable conductivity) and varying sizes in real-world environments, electric field distribution and droplet position are more critical determining factors. This simplifies the overly complex consideration of droplet physical parameters in engineering analysis.

The study's implications for external insulation design of power equipment clarify that water droplets significantly reduce the breakdown voltage of air gaps in highly non-uniform electric fields, with the reduction effect intensifying as the gap length increases. In designing air gaps for high-voltage transmission lines, insulators, and similar equipment, the impact of water droplets under humid conditions—such as rain, fog, and condensation—must be fully considered. Optimizing electrode shapes and layouts is essential to mitigate the risk of unexpected flashover caused by electric field distortion induced by water droplets.

Author Contributions: Conceptualization, J.Z. (Jianli Zhao) and B.C.; Methodology, J.Z. (Jianli Zhao), Z.D. and B.C.; Formal analysis, J.Z. (Jianli Zhao), Z.D. and B.C.; Investigation, J.Z. (Jianli Zhao), Z.D., J.Z. (Jiankun Zhao) and S.F.; Resources, J.Z. (Jiankun Zhao); Data curation, J.Z. (Jianli Zhao), Z.D., J.Z. (Jiankun Zhao) and S.F.; Writing—original draft, J.Z. (Jianli Zhao); Writing—review & editing, J.Z. (Jianli Zhao), Z.D., J.Z. (Jiankun Zhao), S.F. and B.C.; Visualization, J.Z. (Jianli Zhao); Supervision, B.C.; Project administration, B.C. All authors have read and agreed to the published version of the manuscript.

Funding: This work was supported by the 2024 Science and Technology Program of Inner Mongolia Power (Group) Co., Ltd., under the project "Research on Comprehensive Mitigation Technologies for Bird-Related Faults in Transmission Lines" (Project No. 2024-4-52). The APC was funded by Inner Mongolia Power (Group) Co., Ltd.

Data Availability Statement: The data presented in this study are available on request from the corresponding author.

Conflicts of Interest: Authors Jianli Zhao and Jiankun Zhao are employed by Inner Mongolia Power (Group) Co., Ltd. The remaining authors declare that the research was conducted in the absence of any commercial or financial relationships that could be construed as a potential conflict of interest.

References

1. Zhang, C.; Wang, L.; Guan, Z. Investigation of DC discharge behavior of polluted porcelain post insulator in artificial rain. *IEEE Trans. Dielectr. Electr. Insul.* **2016**, *23*, 331338. [CrossRef]
2. McDermid, W.; Black, T. Experience with preventing external flashovers in HVDC converter stations. In Proceedings of the Conference Record of the 2008 IEEE International Symposium on Electrical Insulation, Vancouver, BC, Canada, 9–12 June 2008; pp. 81–84.
3. Rizk, F.A.; Kamel, S.I. Modelling of HVDC wall bushing flashover in nonuniform rain. *IEEE Trans. Power Deliv.* **1991**, *6*, 1650–1662. [CrossRef]
4. Hartings, R. The ACbehavior of a hydrophilic and hydrophobic post insulator during rain. *IEEE Trans. Power Deliv.* **2002**, *9*, 1584–1592. [CrossRef]
5. Yang, L.; Kuang, Z.; Sun, Y.; Liao, Y.; Hao, Y.; Li, L.; Zhang, F. Study on surface rainwater and arc characteristics of highvoltage bushing with booster sheds under heavy rainfall. *IEEE Access* **2020**, *8*, 146865–146875. [CrossRef]
6. Chen, B.H.; Lu, J.Z.; Wang, B.W.; Sun, Y.C.; Wu, C.P.; Deng, J. AC discharge performance of short ballball and rodplate air gaps under water mist conditions. *IEEE Trans. Dielectr. Electr. Insul.* **2020**, *27*, 1068–1075. [CrossRef]
7. Danikas, M.G.; Rakitzis, P.; Karakoulidis, K. Study of parameters related to deterioration phenomena due to water droplets on polymeric surfaces. *J. Electr. Eng.* **2006**, *57*, 130–137.
8. Jiang, X.; Yuan, Y.; Bi, M.; Du, Y.; Ma, J. AC breakdown performance and voltage correction of rodplane short air gap under rain conditions. *IEEE Trans. Dielectr. Electr. Insul.* **2013**, *20*, 515–523. [CrossRef]
9. Hu, Y.; Wang, L.N.; Liu, K.; Shao, G.W.; Liu, T.; Hu, J. Research of effect of windblown rain on power frequency flashover characteristic of conductortower air gap. In Proceedings of the 2009 AsiaPacific Power and Energy Engineering Conference 2009, Wuhan, China, 27–31 March 2009; p. 16.
10. Wu, X.; Cao, B.; Li, Z.; Yang, D.; Shen, S.; Wang, L. DC breakdown characteristic of air gap with water droplets. *IEEE Trans. Plasma Sci.* **2021**, *49*, 1962–1968. [CrossRef]
11. Liu, G.; Lu, H.; Cai, H.; Sun, Z.; Wen, X. Experimental Investigation of Breakdown Characteristics of RodPlateRod Gap Under Impulse Voltage. In Proceedings of the 2020 IEEE 4th Conference on Energy Internet and Energy System Integration (EI2), Wuhan, China, 30 October 2020–1 November 2020; pp. 4064–4069.
12. Taniguchi, S.; Okabe, S.; Asakawa, A.; Shindo, T. Flashover characteristics of long air gaps with negative switching impulses. *IEEE Trans. Dielectr. Electr. Insul.* **2008**, *15*, 399–406. [CrossRef]
13. Jiang, X.; Yuan, Y.; Bi, M.; Du, Y.; Ma, J. DC positive discharge performance of rodplane short air gap under rain conditions. *IEEE Trans. Dielectr. Electr. Insul.* **2013**, *20*, 104–111. [CrossRef]
14. Nazemi, M.H.; Hinrichsen, V. Experimental investigations on water droplet oscillation and partial discharge inception voltage on polymeric insulating surfaces under the influence of AC electric field stress. *IEEE Trans. Dielectr. Electr. Insul.* **2013**, *20*, 443–453. [CrossRef]
15. Swift, D.A. Flashover of an insulator surface in air due to polluted water droplets. In Proceedings of 1994 4th International Conference on Properties and Applications of Dielectric Materials (ICPADM), Brisbane, QLD, Australia, 3–8 July 1994; Volume 2, pp. 550–553.
16. Jie, D.; Baohui, C.; Qiang, H.; Yingwei, Y.; Kai, X. Influence of Water Film Over Sphere Sphere Electrodes on Power Frequency Discharge Characteristics of Air Gap. In Proceedings of the 2019 IEEE 3rd Conference on Energy Internet and Energy System Integration (EI2), Changsha, China, 8–10 November 2019; pp. 2429–2432.
17. Li, Q.; Rowland, S.M.; Dupere, I.; Morris, R.S. The impact of water droplet vibration on corona inception on conductors under 50 Hz AC fields. *IEEE Trans. Power Deliv.* **2018**, *33*, 2428–2436. [CrossRef]

18. Yuan, Y.; Jiang, X.; Rowland, S.M.; Xiao, A.; Li, Q.; Wang, S. Calculations of breakdown voltage of rodplane air gaps in the presence of water streams. *IEEE Trans. Dielectr. Electr. Insul.* **2015**, *22*, 1577–1587. [CrossRef]
19. Liu, Q.; Yang, L.; Hao, Y.; Li, L.; Ding, J.; Hu, X. Numerical study of breakdown voltage calculation and discharge characteristics of millimeterlevel short air gap with a single water droplet. *Plasma Sources Sci. Technol.* **2024**, *33*, 125015. [CrossRef]

Disclaimer/Publisher's Note: The statements, opinions and data contained in all publications are solely those of the individual author(s) and contributor(s) and not of MDPI and/or the editor(s). MDPI and/or the editor(s) disclaim responsibility for any injury to people or property resulting from any ideas, methods, instructions or products referred to in the content.